Bioorganic Chemistry 87 (2019) 366–372

Contents lists available at ScienceDirect

Bioorganic Chemistry

journal homepage: www.elsevier.com/locate/bioorg

Synthesis of TPEN variants to improve cancer cells selective killing capacity

Stephanie Schaefer-Ramadan[a], Maciej Barlog[b], Jim Roach[c], Mohammed Al-Hashimi[b], Hassan S. Bazzi[b], Khaled Machaca[a,*]

[a] Department of Physiology and Biophysics, Weill Cornell Medicine – Qatar, Doha, Qatar
[b] Department of Chemistry, Texas A&M University at Qatar, P.O. Box 23874, Doha, Qatar
[c] Pre-Medical Education, Weill Cornell Medicine – Qatar, Doha, Qatar

ARTICLE INFO

Keywords:
TPEN
Transition metals
ROS
Cancer
Cell death

ABSTRACT

TPEN is an amino chelator of transition metals that is effective at the cellular and whole organism levels. Although TPEN of often used as a selective zinc chelators, it has affinity for copper and iron and has been shown to chelate both biologically. We have previously shown that TPEN selectively kills colon cancer cells based on its ability to chelate copper, which is highly enriched in colon cancer cells. The TPEN-copper complex is redox active thus allowing for increased ROS production in cancer cells and as such cellular toxicity. Here we generate TPEN derivatives with the goal of increasing its selectivity for copper while minimizing zinc chelation to reduce potential side effects. We show that one of these derivatives, TPEEN despite the fact that it exhibits reduced affinity for transition metals, is effective at inducing cell death in breast cancer cells, and exhibits less toxicity to normal breast cells. The toxicity effect of the both chelators coupled to the metal content of the different cell types reveals that they exhibit their toxicity through chelating redox active metals (iron and copper). As such TPEEN is an important novel chelators that can be exploited in anti-cancer therapies.

1. Introduction

N,N,N′,N′-tetrakis(2-pyridylmethyl)-1,2-ethanenediamine (TPEN) belongs to the family of acyclic amino chelators that exhibit a high affinity for transition metals based on their ethylene diamine ligand group [7]. TPEN has six amino donor groups including two aliphatic amino nitrogens and four heterocyclic nitrogens making it a potential hexadentate ligand. TPEN is capable of freely crossing biological membranes and chelates copper, zinc and iron with high efficiency. Nonetheless, most functional studies employ TPEN as a selective zinc chelators while minimizing its de facto role of binding and chelating other transition metals [6,8,13,14]. These reports argue that the observed phenotype, which is mostly the induction of cell death by apoptosis following TPEN treatment, is due to zinc chelation while ignoring potential effects that may arise following the chelation of other transition metals. In fact, TPEN has been shown to effectively chelate and deplete copper from HL-60 cells [15]. This is an important consideration given that the stability constant in solution for the TPEN-Cu^{2+} complex (20.5) is significantly higher than that for the TPEN-Zn^{2+} complex (15.5), with the stability constant for the TPEN-Fe^{3+} iron complex at 14.6 [1]. Therefore, at the cellular level TPEN is likely to chelate all three transition metals with significant efficiency. There is at least one report that argues that in the brain TPEN may show selectivity for zinc over copper [2].

Supporting the above argument, Fatfat et al. argued that TPEN treatment of colon cells causes apoptosis by chelating copper and allowing it to redox cycle within the complex [9]. Normal colon epithelial cells were able to tolerate TPEN concentrations on the order of 5 μM, concentrations that led to significant cell death in colon cancer cells. This selective killing was shown to be due to the fact that colon cancer cells accumulate copper to significantly higher levels than that of normal cells. TPEN effectively strips copper from cellular proteins and its redox cycling within the TPEN-copper complex results in reactive oxygen species (ROS) generation. With higher levels of copper in colon cancer cells, their treatment with TPEN leads to higher levels of ROS and explains the selective toxicity observed [9]. In contrast to copper, zinc is not redox active and as such does not contribute to the generation of ROS. However, zinc chelation will have deleterious effects. We were therefore interested in modifying TPEN to increase its selectivity for copper while minimizing zinc chelation.

From the crystal structures of TPEN [4] we know that TPEN has 6 possible donor groups. In order for TPEN to sequester Zn^{2+} or Fe^{2+} all 6 of the donor groups are used, but Cu^{2+} is chelated by only 5 of the possible 6 donor groups. Using this premise, we sought to make TPEN

* Corresponding author at: Weill Cornell Medicine in Qatar, Education City, Qatar Foundation, P.O. Box 24144, Doha, Qatar.
E-mail address: khm2002@qatar-med.cornell.edu (K. Machaca).

https://doi.org/10.1016/j.bioorg.2019.03.045
Received 27 August 2018; Received in revised form 28 January 2019; Accepted 15 March 2019
Available online 16 March 2019
0045-2068/

derivatives which could preferentially bind Cu^{2+} by removing one of the four pyridine rings of TPEN and replacing it with an ethyl or methyl group or by increasing the linker length to try and disrupt metal binding ability.

2. Materials and methods

2.1. Materials

TPEN (Cat. P4413) and Luperox TBH70X (tert-Butyl hydroperoxide solution, TBHP, Cat. 458139) were purchased from Sigma Aldrich. 2-(Chloromethyl)pyridine hydrochloride (98%) and amines used were purchased from Sigma Aldrich. All reagents were used without further purification. WST1 was purchased from Roche Life Sciences (SKU 5015944001). CellRox Deep Red was purchased from Life Technologies (Cat. C10422). CMH_2DCMDA was purchased from Thermo Fisher (Cat. C6827).

2.2. Cell lines and culture

Human mammary epithelial cells (HMEC) cells were purchased from Lonza and grown using media recommended by the manufacturer utilizing low passage number. MCF7 and MDA-MB231 cells are from ATCC and grown with DMEM supplemented with 10% FBS and 1% Penicillin Streptomycin.

2.3. Spectrophotometry of TPEN and TPEEN

Spectra were recorded using a Cary 5000 UV-Vis-NIR Spectrophotometer with a semi-micro quartz cuvette with a final reaction volume of 450 µL. A 1 mM stock of TPEN or TPEEN was made in 100% ethanol and stored at −20 °C. 50 µM TPEN or TPEEN dilution was made in 20 mM Tris pH 7.5. A 1 mM stock concentration of $CuCl_2$ was made in 20 mM Tris pH 7.5.

2.4. WST1 cell death assay

7×10^3 to 1×10^4 of HMEC, MCF7 and MDA-MB-231 cells were plated per well of a 96-well plate. One experiment consisted of 7 replicates for each TPEN concentration that were averaged. Consistently, with all cell lines and TPEN compounds, there are some wells that fail to react with the WST1 because the cells in the well are already dead prior to incubation. For this reason, replicates outside of 1 standard deviation were discarded in the averaging. Each experiment was repeated at least 3 times. 100 mM stocks of TPEN or TPEEN were made in 100% ethanol and stored at −20 °C. 1 mM working stocks of these compounds were made fresh by dilution into cell culture media. The media was removed from all wells and replaced with fresh media supplemented with the appropriate [TPEN] or [TPEEN]. Cells were incubated for 24 h after which 10 µL of WST1 was added directly into each well (in the dark) followed by a 1 h incubation at 37 °C. The WST1 compound is light sensitive so the 96 well plate is covered in foil during the incubation period. The absorbance is measured directly between 420 and 480 nm with a reference wavelength at 600 nm. The blank for this experiment is media (no cells) plus WST1. The control well is media plus 0.1% ethanol and WST1. The following equation was used to calculate % viability of the cells:

$$\%\ Viability = \frac{Abs(420\ \text{nm} - 600\ \text{nm}) - blank}{blank - control} * 100$$

2.5. Measuring ROS generation in cell lines.

HMEC, MCF7 and MDA-MB-231 cells were treated with 12.5 µM CellRox Deep Red or 10 µM CM-H_2DCFDA florescent dyes in the presence or absence of 10 µM TPEN or 10 µM TPEEN. The increase in fluorescence indicates an environment that has more ROS. TPEN or TPEEN were added at the same time as the dye for a total incubation of 45 min. The CM-H_2DCFDA dye was reconstituted in 100% ethanol and incubated with the cells (± TPEN or ± TPEEN) in PBS where the CellRox Deep Red dye is compatible in complete media. Cells were trypsinized after the 45 min incubation time and washed with PBS. 300 µL of PBS was added to the washed cell pellets for FACS analysis. TBHP positive control was used at a final concentration of 100 µM.

2.6. Inductively coupled mass spectroscopy

Cell pellets were analyzed by University of Nebraska-Lincoln as previously described [16].

3. Synthesis of TPEN derivatives

The following procedure was modified from [3].

***N^1*-ethyl-*N^1*,*N^2*,*N^2*-tris(pyridin-2-ylmethyl)ethane-1,2-diamine** (TPMEN): *N*-ethyl diamine (550 mg, 6.24 mmol) was dissolved in CH_2Cl_2 (10 mL). Chloromethyl pyryidine HCl salt (3.07 g, 18.71 mmol) was added followed by water (10 mL). Solution of NaOH in water (1.8 g in 6 mL) was added drop wise and the reaction mixture was stirred at RT for 3 days. Water (50 mL) was added and product was extracted with CH_2Cl_2 (3 × 20 mL), dried over $MgSO_4$, solvent volume reduced to ca. 10 mL under vacuum and transferred to short chromatographic column and purified with EtOAc/MeOH gradient (0–30% MeOH). All products were isolated as viscous orange oils.

***N^1*-ethyl-*N^1*,*N^2*,*N^2*-tris(pyridin-2-ylmethyl)ethane-1,2-diamine** (TPMEN): **^{1}H** NMR (400 MHz, $CDCl_3$, supporting figure 1) δ 0.90 (t, J = 7.0 Hz, 3H), 2.43 (q, J = 7.0 Hz, 2H), 2.62 (s, 4H), 3.61 (s, 2H), 3.74 (s, 4H), 6.99–7.04 (m, 3H), 7.30–7.54 (m, 6H), 8.38–8.41 (m, 8H). **^{13}C** NMR (100 MHz, $CDCl_3$, supporting figure 2) δ 11.7 (CH_3), 48.1 (CH_2-N), 51.6 (CH_2-N), 52.1 (CH_2-N), 60.1 (CH_2-Py), 60.6 (2xCH_2-Py), 121.5 (C), 121.6 (2xC), 122.6 (3xCH), 136.0 (CH), 136.1 (2xCH), 148.6 (CH), 148.7 (2xCH), 159.6 (2xCH), 160.1 (CH). 2.05 g (91%), orange oil.

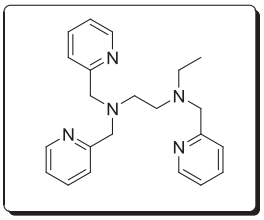

***N^1*-methyl-*N^1*,*N^2*,*N^2*-tris(pyridin-2-ylmethyl)ethane-1,2-diamine** (TPEEN): **^{1}H** NMR (600 MHz, $CDCl_3$, supporting figure 3) δ 2.06 (s, 3H), 2.52 (t, J = 6.6 Hz, 2H), 2.63 (t, J = 6.7 Hz, 2H), 3.50 (s, 2H), 3.71 (s, 4H), 6.97 (br. s, 3H), 7.22 (d, J = 7.8 Hz, 1H), 7.37–7.48(m, 5H), 8.35 (br. s, 3H). **^{13}C** NMR (125 MHz, $CDCl_3$, supporting figure 4) δ 42.5 (CH_3-N), 51.8 (CH_2-N), 55.2 (CH_2-N), 60.4 (2xCH_2-Py), 63.7 (CH_2-Py), 121.5 (3xCH), 122.5 (2xC), 122.6 (C), 135.97 (CH), 135.99 (2xCH), 148.57 (2xCH), 148.59 (CH), 158.9 (CH), 159.4 (2xCH). 1.75 g (86%), orange oil.

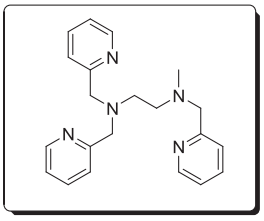

***N^1*-methyl-*N^1*,*N^2*,*N^2*-tris(pyridin-2-ylmethyl)propane-1,3-diamine** (TPEPN): **^{1}H** NMR (600 MHz, $CDCl_3$, supporting figure 5) δ 1.73–1.76 (m, 2H), 2.17 (s, 3H), 2.41 (t, J = 7.3 Hz), 2.57 (t,

J = 7.2 Hz, 2H), 3.58 (s, 2H), 3.78 (s, 4H), 7.09–7.10(m, 3H), 7.29 (d, 7.8 Hz, 1H), 7.45–7.60 (m, 5H), 8.47 (m, 3H). **^{13}C** NMR (125 MHz, $CDCl_3$, supporting figure 6) δ 24.8 (CH_2), 42.3 (CH_3), 52.4 (CH_2-N), 55.6 (CH_2-N), 60.4 (2xCH_2-Py), 63.6 (CH_2-Py), 121.81 (C), 121.83 (2xC), 122.8 (2xCH), 123.0(CH), 136.30 (2xCH), 136.32 (CH), 148.81 (2xCH), 148.84 (CH), 159.3 (CH), 159.8 (2xCH). 1.59 g (75%) orange oil.

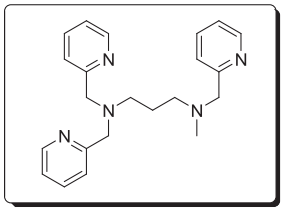

3.1. Stability constant determinations

The stability constants (β) for TPMEN, TPEEN, and TPEPN with Cu^{2+}, Zn^{2+}, and Fe^{2+} were determined spectrophotometrically using the competitive method described previously by [12]. The method establishes the stability constant a ligand-metal complex relative to that of another complex for which the stability constant is known. Anderegg et al. determined that the stability constant for the complex of N,N,N′,N′-tetrakis(2-pyridinylmethyl)-1,2-ethanediamine and Cu^{2+} ($[Cu(TPEN)]^{2+}$) is 3.5×10^{20} or $log\,(\beta_{Cu-TPEN}) = 20.54$ [1]. Using TPEN as the competing ligand against TPMEN for Cu^{2+}, a series of solutions were prepared of known total TPEN concentration (C_{TPEN}), total TPMEN concentration (C_{TPMEN}), and total Cu^{2+} concentration (C_{Cu}). Spectrophotometric analysis of these solutions at 300 nm provided data from which $\beta_{Cu-TPMEN}$ was elucidated. For a pair of solutions of different ligand and/or metal concentration, Solutions 1 and 2, absorbance values at 300 nm (A_{300-1}) and (A_{300-2}) were measured using an Agilent 8453 spectrophotometer and a 1 cm quartz cuvette. All solutions contained 0.10 M KCl and were brought into the pH range 6.0–6.5 through addition of 0.1 M KOH. As shown in Eqs. (1) and (2), absorbance values at this wavelength are assumed to functions of only the molar absorptivities for Cu-TPEN ($\epsilon_{Cu-TPEN}$) and Cu-TPMEN ($\epsilon_{Cu-TPMEN}$) and their respective equilibrium concentrations, $[Cu-TPEN]$ and $[Cu-TPMEN]$.

$$A_{300-1} = \epsilon_{Cu-TPEN}\,[Cu-TPEN]_1 + \epsilon_{Cu-TPMEN}\,[Cu-TPMEN]_1 \quad (1)$$

$$A_{300-2} = \epsilon_{Cu-TPEN}\,[Cu-TPEN]_2 + \epsilon_{Cu-TPMEN}\,[Cu-TPMEN]_2 \quad (2)$$

Eqs. (3)–(5) provide typical mass-balance expressions for Solution 1, where $[Cu^{2+}]$ is the concentration of free metal, $[TPEN]$ is the concentration of free TPEN, and $[TPMEN]$ is the concentration of free TPMEN. Analogous relationships for Solution 2 are provided in Eqs. (6)–(8).

$$C_{TPEN-1} = [TPEN]_1 + [Cu-TPEN]_1 \quad (3)$$

$$C_{TPMEN-1} = [TPMEN]_1 + [Cu-TPMEN]_1 \quad (4)$$

$$C_{Cu-1} = [Cu^{2+}]_1 + [Cu-TPEN]_1 + [Cu-TPMEN]_1 \quad (5)$$

$$C_{TPEN-2} = [TPEN]_2 + [Cu-TPEN]_2 \quad (6)$$

$$C_{TPMEN-2} = [TPMEN]_2 + [Cu-TPMEN]_2 \quad (7)$$

$$C_{Cu-2} = [Cu^{2+}]_2 + [Cu-TPEN]_2 + [Cu-TPMEN]_2 \quad (8)$$

The stability constant expressions for Solutions 1 and 2 are provided in Eqs. (9) and (10), where $\beta_{Cu-TPMEN}$ is the stability constant for the Cu-TPMEN complex.

$$\beta_{Cu-TPEN} = \frac{[Cu-TPEN]_1}{[Cu^{2+}]_1[TPEN]_1} = \frac{[Cu-TPEN]_2}{[Cu^{2+}]_2[TPEN]_2} \quad (9)$$

Table 1
Ligand-metal stability constants.

	log (β)		
Ligand	Cu^{2+}	Zn^{2+}	Fe^{2+}
TPEN[a]	20.5 ± 0.1	15.6 ± 0.1	14.6 ± 0.1
TPMEN	19.0 ± 0.2	13.3 ± 0.2	11.9 ± 0.2
TPEEN	19.1 ± 0.2	12.9 ± 0.2	11.7 ± 0.3
TPEPN	19.0 ± 0.3	11.7 ± 0.2	11.0 ± 0.4

[a] Data from [1].

$$\beta_{Cu-TPMEN} = \frac{[Cu-TPMEN]_1}{[Cu^{2+}]_1[TPMEN]_1} = \frac{[Cu-TPMEN]_2}{[Cu^{2+}]_2[TPMEN]_2} \quad (10)$$

A least-squares analysis of this system of equations, performed using SEQS 3.1 distributed by CET Research Group, provides $\beta_{Cu-TPMEN}$.

Once $\beta_{Cu-TPMEN}$ had been determined, the same competition method, in the first case between TPMEN for both Cu^{2+} and Zn^{2+}, and in the second between TPMEN for both Zn^{2+} and Fe^{2+}, was used to establish $\beta_{Zn-TPMEN}$ and $\beta_{Fe-TPMEN}$. Similarly, $\beta_{Cu-TPEEN}$ and $\beta_{Cu-TPEPN}$ were determined by competition between the respective ligands and TPEN for Cu^{2+}. Subsequent experiments were then performed to ascertain stability constants for the Zn^{2+} and Fe^{2+} complexes.

4. Results and discussion

4.1. Stability constants of TPEN and TPEN derivatives

Our first goal was to characterize the affinity each TPEN derivative had for Cu^{2+}, Zn^{2+} and Fe^{2+} and compare them to TPEN. Table 1 shows the ligand-metal stability constants for the three TPEN derivatives used in this study. Ultimately, our goal was to modify TPEN in a way that we could either increase the affinity for Cu^{2+} or decrease the affinity for Zn^{2+} and Fe^{2+}.

Interactions between TPMEN, TPEEN, and TPEPN and the metals investigated are quite strong. Although the ligands investigated lack a 2-pyridylmethyl moiety when compared to TPEN, previous studies have reported that the coordination number for Cu^{2+} in $[Cu(TPEN)]^{2+}$ is only five [1,11]. It is perhaps not surprising, therefore, that the chelate stabilities of the Cu^{2+} complexes are closer to that of TPEN when compared to the corresponding Zn^{2+} and Fe^{2+} complexes. The small differences in stability constants between TPMEN and TPEEN are within the experimental errors. If genuine, these dissimilarities are likely a result of the competing effects of slightly increased basicity at the amino nitrogen for the ethyl substituent compared to the methyl versus the somewhat reduced steric hindrance of metal chelation for the methyl compared to the ethyl. The additional methylene group between the amino nitrogens in TPEPN produces a six-member chelation ring, compared to five-member rings in the other ligands investigated. The increased ring size leads to reduced stability for the Zn^{2+} and Fe^{2+} complexes, while the stability of the Cu^{2+} complex appears unaffected. A similar trend was observed in the stabilities of ethylenediaminetetraacetic acid (EDTA) metal complexes when compared to those of trimethyleneaminetetraacetic acid (TMDTA), with stability constants observed to generally decrease as ionic radius increases [10]. Stability constants for complexes of the pentadentate ligand N,N,N′-tris(2-pyridylmethyl)-N′-benzyl-1,2-ethanenediamine (BnTPEN) with Zn^{2+} [17] and Fe^{2+} [12] have been determined previously to be 1×10^{15} and 5×10^{13}, respectively. Both values are higher than those obtained for similar complexes in this study. Interestingly, Bruno et al. observed that benzyl-substituted ethylenediaminetriacetic acid had a larger stability constant with Cu^{2+} than did various alkyl-substituted analogs by approximated four orders of magnitude [5].

Both the TPMEN and TPEEN derivatives have nearly identical stability constants for Cu^{2+}, Zn^{2+} and Fe^{2+}. Therefore, we selected

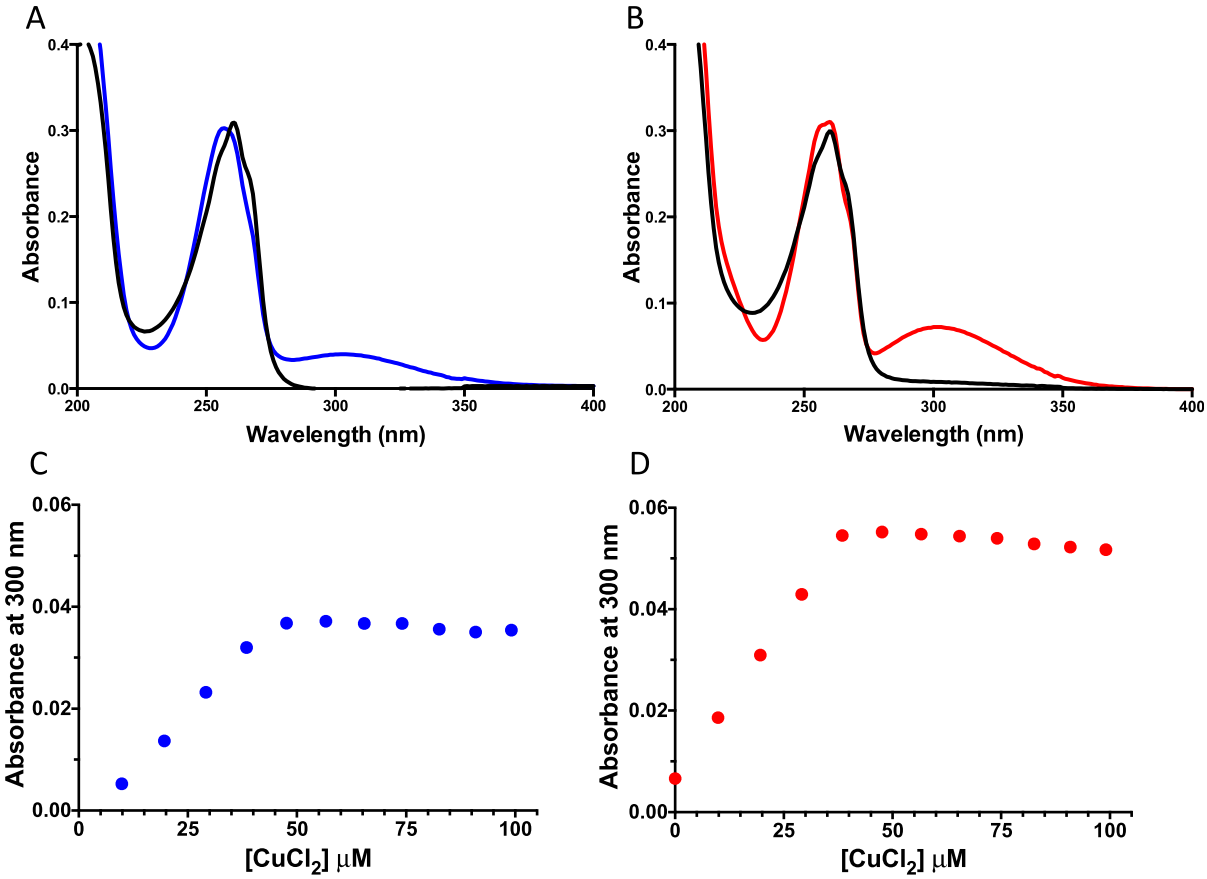

Fig. 1. UV–VIS spectra of TPEN and TPEEN. (A) 50 μM TPEN (black) plus the addition of 47.6 μM $CuCl_2$ (blue) and (B) 50 μM TPEEN (black) plus the addition of 47.6 μM $CuCl_2$ (red). (C) and (D) Titration plot of TPEN and TPEEN, respectively, showing the addition of increasing amounts of $CuCl_2$. Absorbance for panels C and D were measured at 300 nm. All spectra were recorded in 20 mM Tris pH 7.5.

TPEEN for further characterization studies. The TPEN derivative, TPEPN, precipitates at higher pH and was not pursued for further studies. Fig. 1 shows spectrophotometric analysis of TPEN and TPEEN in the presence and absence of Cu^{2+}. Fig. 1A shows 50 μM TPEN before (black) and after the addition of 47.6 μM $CuCl_2$ (blue). We observe an increased absorbance with λ_{max} at 302 nm and shows approximate 1:1 stoichiometry as demonstrated by the titration plot in Fig. 1C. Similarly, we observe an increased absorbance at 302 nm with the TPEEN derivative upon the addition of 47.6 μM $CuCl_2$ (Fig. 1B, red) under the same conditions. Again, the TPEEN derivative also demonstrates approximate 1:1 binding with the Cu^{2+} ligand (Fig. 1D).

4.2. Characterizing TPEEN

For this study we tested the cytotoxic effects of TPEN and TPEEN on normal breast cells, HMEC, as well as two breast cancer cell lines, MCF7 and MDA-MB-231. When compared to TPEN, the TPEEN compound was able to kill the MCF7 and MDA-MB-231 cells with nearly equal efficiency as TPEN itself (Fig. 2). However, both TPEN and TPEEN have a slightly lower IC_{50} values for the normal breast cells when compared to the two cancerous breast cell lines (Fig. 2 table inset), with the difference being for TPEEN the IC_{50} for the normal and cancerous cell lines are similar. Another important difference between TPEN and TPEEN is the level of toxicity reached at maximal concentrations of the chelators. Whereas TPEN even at the highest concentrations used was able to kill a maximum of around 75% of the population of cancerous breast cells (Fig. 2A), TPEEN was significantly more effective at the levels of killing reaching close to 90% of the population (Fig. 2B).

4.3. Metal analysis of cell lines

Our initial hypothesis for generating these TPEN derivatives was to see if we could have a selective Cu^{2+} chelator since previous work showed that NCM460 colon cells had 5 times less Cu^{2+} than the cancerous HCT116 cells [9]; and TPEN had a lower IC_{50} value for HCT116 cells than for the normal NCM460 cells with values of 8.3 μM and 13 μM, respectively. These data along with others from Fatfat et al. support the hypothesis that cancerous cells have more copper than their normal counterparts and this is the reason TPEN is more effective at killing in cancerous cells vs. normal cells.

We then measured the transition metal content of normal breast cells (HMEC) as well as MCF7 and MDA-MD-231 cell samples using ICP-MS (Fig. 3). These data show that the cancerous breast cells, similar to what is observed in colon cells, have more Cu^{2+} than the normal breast cells. However, in contrast to what is observed in colon cancer cells the susceptibility of the three cell lines in the cell death assay (Fig. 2) does not correlate with their copper content, since the normal HMEC cells have a lower IC_{50} than both of the cancerous breast cell lines, yet it has the lowest copper content (Figs. 2 and 3). Surprisingly though, the HMEC cell line had significantly higher iron levels as compared to the two cancerous cell lines MCF7 and MDA-MB-231 (Fig. 3). Just as for copper, iron is redox active and would contribute to ROS-mediated toxicity following TPEN or TPEEN treatment. The higher sensitivity of HMEC cells to chelator treatment can thus be explained by the higher levels of redox active metals (copper and iron combined) as compared to MCF7 and MDA-MB-231 cells (Fig. 4). In the previously published work of Fatfat et al., the Fe^{2+} levels of both the HCT116 and NCM460 cells were very similar [9]. Therefore, the sum of copper and iron in the

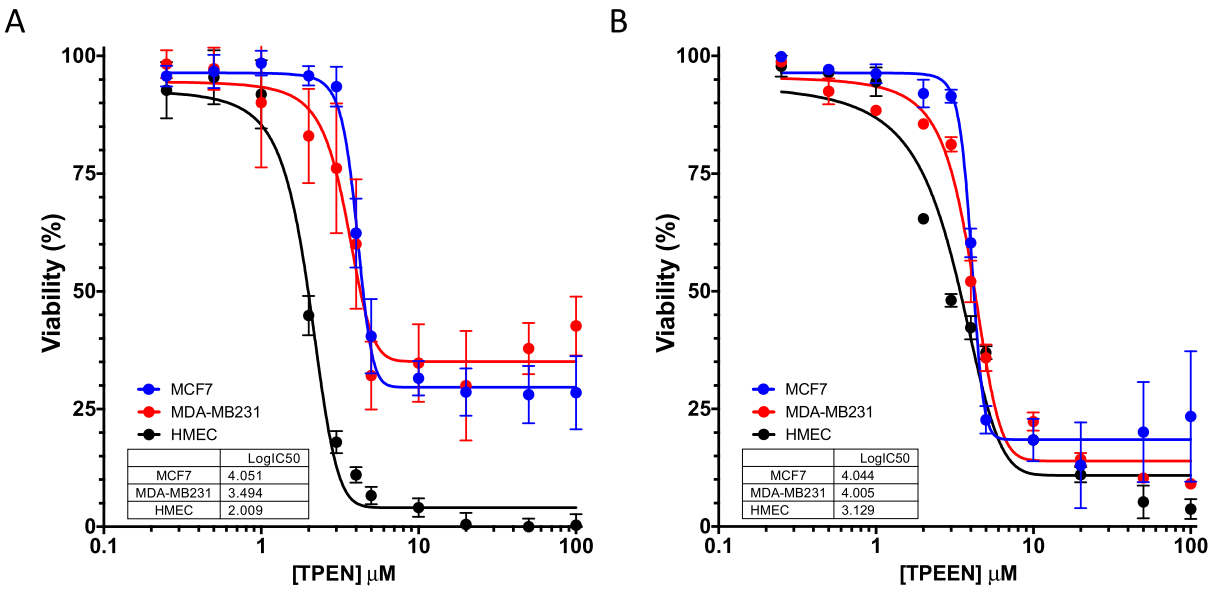

Fig. 2. WST1 assay using TPEN and TPEEN. Testing viability of HMEC (black), MCF7 (blue) and MDA-MD-231 (red) cells using TPEN (panel A) and TPEEN (panel B). Experiments were performed in triplicate and error bars represent SD. The Log IC_{50} values are shown as an inset in each panel.

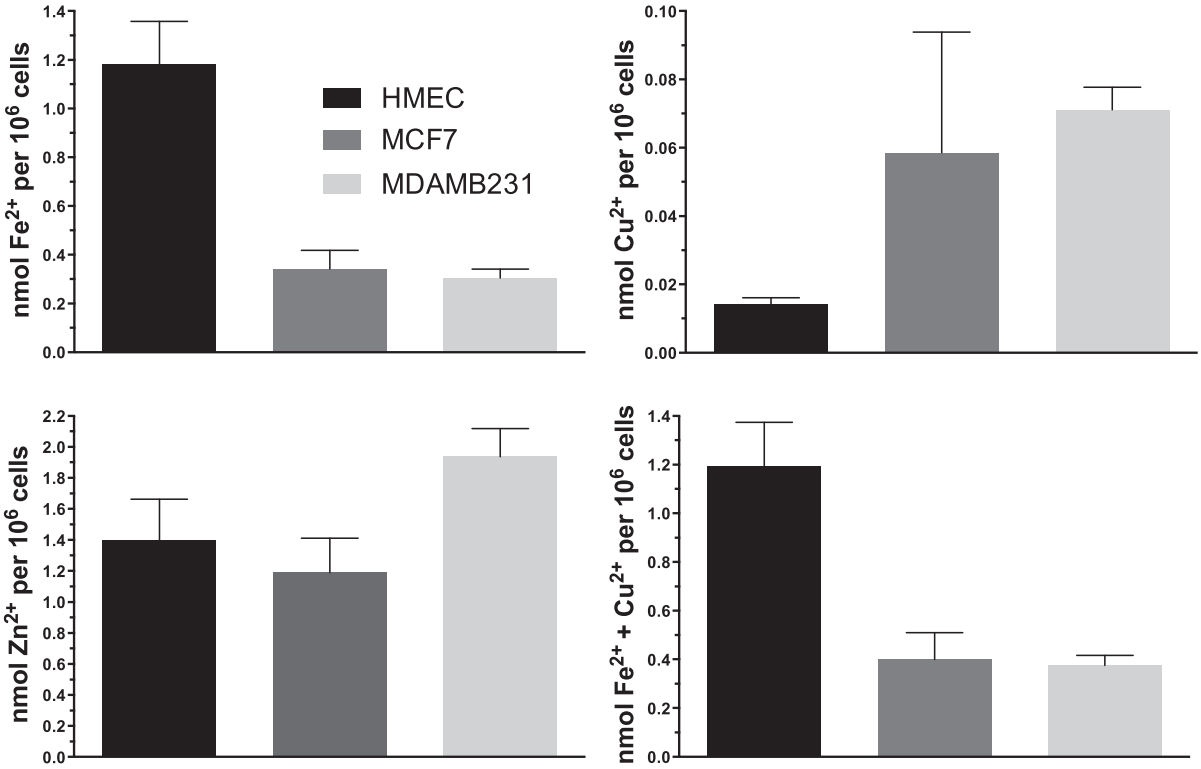

Fig. 3. Metal analysis of cell lines used in this study. ICP-MS results were calculated as published previously [16]. Values are reported as nmol metal per 10^6 cells. Error bars represent SD of at least three replicates.

HCT116 cells is significantly higher than NCM460, explaining their higher susceptibility to TPEN. In the cell lines tested in this manuscript, the mean Fe^{2+} level in the HMEC (1.18 nmol/10^6 cells) is over three-fold higher than the level in MCF7 and MDA-MB-231 cells lines (Fig. 3). Similarly, HCT116 cells from our lab contained a mean value of 1.56 nmol Fe^{2+}/10^6 cells with IC_{50} value of 3.72 μM when treated with TPEN for 24 h (data not shown).

4.4. Inducing cellular ROS with TPEN or TPEEN

Previous work demonstrated that reduction of TPEN-Fe^{3+} to TPEN-Fe^{2+} and TPEN-Cu^{2+} to TPEN-Cu^{1+} complexes by ascorbic acid were redox active and generate hydroxide radical and superoxide anion radical, respectively [9]. To test the ability of TPEEN to generate reactive oxygen species, we incubated cells with 10 μM TPEN or TPEEN (45 min)

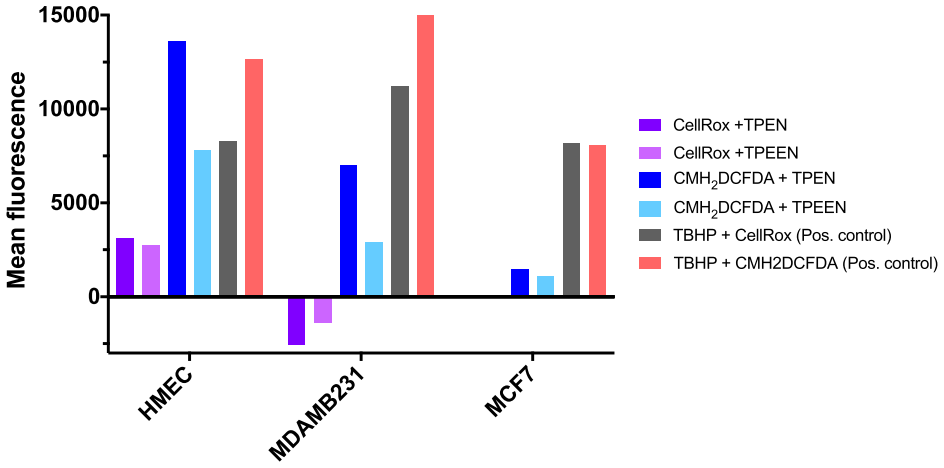

Fig. 4. ROS generation in cell lines treated with TPEN or TPEEN using two different dyes for ROS detection. HMEC, MCF7 and MDA-MB-231 cells were treated with CellRox Deep Red or CM-H_2DCFDA florescent dyes for 45 min in the presence or absence of TPEN or TPEEN. TBHP acts as a positive control.

Table 2
ROS properties of CellRox Deep Red and CM-H_2DCFDA dye.

	Hydrogen peroxide (H_2O_2)	Hydroxyl radical ($HO^{\cdot}$)	Hypochlorous acid (HOCl)	Nitric oxide (NO)	Peroxyl radical ($ROO^{\cdot}$)	Peroxynitrite anion ($ONOO^-$)	Singlet oxygen ($^1O_2$)	Superoxide anion ($^{\cdot}O_2^-$)
CellRox Deep Red		+						+
CM-H_2DCFDA	+	+			+	+		

in the presence of either CellRox Deep Red or CM-H_2DCFDA. Both of these dyes are able to detect ROS but they detect different types. Table 2 shows the CM-H_2DCFDA dye is able to detect hydrogen peroxide (H_2O_2), hydroxyl radical ($HO^{\cdot}$), peroxyl radical ($ROO^{\cdot}$), and peroxynitrite anion ($ONOO^-$) where the CellRox Deep Red reagent detects hydroxyl radicals and superoxide anion ($^{\cdot}O_2^-$) (ThermoFisher scientific Reactive oxygen species, Table 18.1).

Figure 4 illustrates the FACS analysis which shows relatively low levels of hydroxide radical and superoxide anion being produced with TPEN and TPEEN in HMEC cells and little to none in MDA-MB-231 and MCF7 cells. The data also indicate that TPEN is able to induce more ROS than TPEEN under the same conditions. These results are consistent with the metal content analyses and the conclusion that the chelators generate ROS by chelating both copper and iron in these cells and would explain why we see a lower IC_{50} for TPEN in the HMEC than for TPEEN.

5. Conclusions

We generate a novel TPEN derivative TPEEN by removing one of the pyridine rings. TPEEN is as effective as TPEN in inducing cancer cell death and exhibits less toxicity to normal breast cells. The toxicity effect of the both chelators coupled to the metal content of the different cell types reveals that they exhibit their toxicity through chelating redox active metals (iron and copper). This is an important finding that could be used to target cancer cells differentially using metal chelators. We were however not able to generate a TPEN derivative that could specifically sequester Cu^{2+} by removing one of the pyridine rings of TPEN. This may not be surprising given the multiple amino donor groups within TPEEN and the flexibility of the molecular in coordinating metals. The similar effectiveness of TPEEN in cell killing further argues that the slightly lower affinity to metals achieved by removing the pyridine ring is advantageous in a cellular context.

Acknowledgements

We would like to thank Aleksandra M. Liberska for her help with the FACS experiments. Funding was generously provided by both the Qatar Foundation (BMRP program to Weill Cornell Medicine) with additional support from the Qatar National Research Fund NPRP 09-047-3-012. The statements made herein are solely the responsibility of the authors and the funders had no role in study design, data collection and analysis, decision to publish, or preparation of the manuscripts.

Appendix A. Supplementary material

Supplementary data to this article can be found online at https://doi.org/10.1016/j.bioorg.2019.03.045.

References

[1] G. Anderegg, E. Hubmann, N.G. Podder, F. Wenk, Pyridine-derivatives as complexing agents. 11. Thermodynamics of metal-complex formation with bis[(2-pyridyl)methyl]-amine, tris[(2-pyridyl)methyl]-amine and tetrakis[(2-pyridyl)methyl]-amine, Helv. Chim. Acta. 60 (1977) 123–140.
[2] C. Armstrong, W. Leong, G.J. Lees, Comparative effects of metal chelating agents on the neuronal cytotoxicity induced by copper (Cu + 2), iron (Fe + 3) and zinc in the hippocampus, Brain Res. 892 (2001) 51–62.
[3] I. Bernal, I.M. Jensen, K.B. Jensen, C.J. Mckenzie, H. Toftlund, J.P. Tuchagues, Iron (Ii) complexes of polydentate aminopyridyl ligands and an exchangeable 6th ligand reactions with peroxides – crystal-structure of [Fel(1)(H2o)][Pf6](2)center-dot-H2o [L(1) = N, N'-bis(6-methyl-2-pyridylmethyl)-N, N'-bis(2-pyridylmethyl)ethane-1,2-diamine], J. Chem. Soc. (1995) Dalton:3667–3675.
[4] C.A. Blindauer, M.T. Razi, S. Parsons, P.J. Sadler, Metal complexes of N, N, N ' N '-tetrakis(2-pyridylmethyl)ethylenediamine (TPEN): variable coordination numbers and geometries, Polyhedron 25 (2006) 513–520.
[5] A.J. Bruno, S. Chaberek, A.E. Martell, The preparation and properties of N-substituted ethylenediaminetriacetic acids, J. Am. Chem. Soc. 78 (1956) 2723–2728.
[6] F. Chai, A.Q. Truong-Tran, A. Evdokiou, G.P. Young, P.D. Zalewski, Intracellular zinc depletion induces caspase activation and p21 Waf1/Cip1 cleavage in human epithelial cell lines, J. Infect. Dis. 182 (2000) S85–S92.
[7] X. Ding, H. Xie, Y.J. Kang, The signifcance of copper chelators in clinical and experimental application, J. Nutr. Biochem. 22 (2011) 301–310.
[8] M. Donadelli, P.E. Dalla, C. Costanzo, M.T. Scupoli, A. Scarpa, M. Palmieri, Zinc depletion efficiently inhibits pancreatic cancer cell growth by increasing the ratio of antiproliferative/proliferative genes, J. Cell Biochem. 104 (2008) 202–212.
[9] M. Fatfat, R.A. Merhi, O. Rahal, D.A. Stoyanovsky, A. Zaki, H. Haidar, V.E. Kagan, H. Gali-Muhtasib, K. Machaca, Copper chelation selectively kills colon cancer cells through redox cycling and generation of reactive oxygen species, BMC Can. 14 (2014) 527.
[10] R.D. Hancock, A.E. Martell, Ligand design for selective complexation of metal-ions in aqueous-solution, Chem. Rev. 89 (1989) 1875–1914.
[11] N. Hirayama, S. Iimuro, K. Kubono, H. Kokusen, T. Honjo, Formation of dinuclear

copper(II) complex with N, N, N', N'-tetrakis(2-pyridylmethyl)-1,2-ethanediamine in aqueous solution, Talanta 43 (1996) 621–626.
[12] C.S. Jackson, J.J. Kodanko, Iron-binding and mobilization from ferritin by polypyridyl ligands, Metallomics 2 (2010) 407–411.
[13] V.M. Kolenko, R.G. Uzzo, N. Dulin, E. Hauzman, R. Bukowski, J.H. Finke, Mechanism of apoptosis induced by zinc deficiency in peripheral blood T lymphocytes, Apoptosis 6 (2001) 419–429.
[14] P. Makhov, K. Golovine, R.G. Uzzo, J. Rothman, P.L. Crispen, T. Shaw, B.J. Scoll, V.M. Kolenko, Zinc chelation induces rapid depletion of the X-linked inhibitor of apoptosis and sensitizes prostate cancer cells to TRAIL-mediated apoptosis, Cell Death. Differ. 15 (2008) 1745–1751.
[15] S.S. Percival, M. Layden-Patrice, HL-60 cells can be made copper deficient by incubating with tetraethylenepentamine, J. Nutr. 122 (1992) 2424–2429.
[16] S. Schaefer-Ramadan, S. Hubrack, K. Machaca, Transition metal dependent regulation of the signal transduction cascade driving oocyte meiosis, J. Cell Physiol. 233 (2018) 3164–3175.
[17] J. Zuo, S.M. Schmitt, Z. Zhang, J. Prakash, Y. Fan, C. Bi, J.J. Kodanko, Q.P. Dou, Novel polypyridyl chelators deplete cellular zinc and destabilize the X-linked inhibitor of apoptosis protein (XIAP) prior to induction of apoptosis in human prostate and breast cancer cells, J. Cell Biochem. 113 (2012) 2567–2575.